

ORKA, The Golden Kaon Experiment: Precision measurement of $K^+ \rightarrow \pi^+ \nu \bar{\nu}$ and other rare processes

E.T. Worcester for the ORKA collaboration^{*†}

Brookhaven National Laboratory

E-mail: etw@bnl.gov

ORKA is a proposed experiment to measure the $K^+ \rightarrow \pi^+ \nu \bar{\nu}$ branching ratio with 5% precision using the Fermilab Main Injector high-intensity proton source. The detector design is based on the BNL E787/E949 experiments, which detected seven $K^+ \rightarrow \pi^+ \nu \bar{\nu}$ candidate events. ORKA is expected to achieve two orders of magnitude improvement in sensitivity relative to the BNL experiments as a result of enhancements to the beam line and the detector acceptance. Precise measurement of the $K^+ \rightarrow \pi^+ \nu \bar{\nu}$ branching ratio with the same level of uncertainty as the well-understood Standard Model prediction allows for sensitivity to new physics at and beyond the LHC mass scale. Detector R&D, simulation-based optimization of the experiment design, and preparation of the experiment location are underway.

2013 Kaon Physics International Conference,

29 April-1 May 2013

University of Michigan, Ann Arbor, Michigan - USA

^{*}Speaker.

[†]ASU, BNL, FNAL, Illinois, INFN-Napoli, INFN-Pisa, INR-Moscow, JINR, Mississippi, Notre Dame, Texas-Arlington, Texas-Austin, TRIUMF, Tsinghua, UBC, UNBC, UASLP

1. Introduction

Precise measurements of rare kaon decay branching ratios provide a window into potential new physics that is complementary to that of direct searches at the energy frontier. Virtual effects in $K^+ \rightarrow \pi^+ \nu \bar{\nu}$ loop diagrams allow us to learn about the flavor- and CP-violating couplings of any new particles that may be discovered at the LHC, and to potentially observe the effects of new particles with masses higher than those accessible by the LHC. The $K^+ \rightarrow \pi^+ \nu \bar{\nu}$ branching ratio in the Standard Model is precisely predicted by theory. The technique to measure the branching ratio experimentally, though challenging, is well-established, and, because seven candidate $K^+ \rightarrow \pi^+ \nu \bar{\nu}$ events have already been seen, a large signal is assured. For these reasons, precision measurement of the $K^+ \rightarrow \pi^+ \nu \bar{\nu}$ branching ratio is an ideal opportunity to test the Standard Model and search for new physics beyond the Standard Model.

The ORKA collaboration proposes to build a stopped-kaon experiment at FNAL to measure the $K^+ \rightarrow \pi^+ \nu \bar{\nu}$ branching ratio with the same uncertainty as the Standard Model prediction, using protons from the Main Injector. Section 2 describes the status of the Standard Model calculation of the $K^+ \rightarrow \pi^+ \nu \bar{\nu}$ branching ratio, and the potential for new physics to affect that branching ratio. The experimental history and current status of the $K^+ \rightarrow \pi^+ \nu \bar{\nu}$ branching ratio measurement are described in Sect. 3. Section 4 describes the BNL E787/E949 experiments on which the ORKA design is based, plans to dramatically improve on the sensitivity of these experiments with ORKA, and the current status of the ORKA experiment. Section 5 is a brief summary.

2. $K^+ \rightarrow \pi^+ \nu \bar{\nu}$ in the Standard Model and Beyond

The branching ratio of the rare $K^+ \rightarrow \pi^+ \nu \bar{\nu}$ decay is theoretically well-understood. The one-loop diagrams for the $s \rightarrow d$ transition are shown in Fig. 1. The calculation is dominated by the top-quark contribution while the charm-quark contribution is significant but controlled. The hadronic matrix element in the expression for the $K^+ \rightarrow \pi^+ \nu \bar{\nu}$ decay rate is shared with that of the $K^+ \rightarrow \pi^0 e^+ \nu_e$ decay, which allows for reliable normalization. The current Standard Model (SM) prediction[1] is

$$B_{SM}(K^+ \rightarrow \pi^+ \nu \bar{\nu}) = (7.8 \pm 0.8) \times 10^{-11}. \quad (2.1)$$

The $\sim 10\%$ uncertainty in Eq. 2.1 makes it one of the most precisely predicted flavor-changing-neutral-current decays involving quarks. This uncertainty is dominated by uncertainties in the CKM matrix; in the near future, improvements to the theory and measurements of the CKM elements are expected to reduce it by a factor of two. Therefore, deviation of the measured decay rate from the SM prediction as small as 35% could be detected with 5σ significance for a measurement with 5% precision.

Many models of new physics predict significant enhancements to the Standard Model branching ratios of $K^+ \rightarrow \pi^+ \nu \bar{\nu}$ and $K_L \rightarrow \pi^0 \nu \bar{\nu}$. This is illustrated in Fig. 2, which shows the range of branching ratio predictions for minimal flavor violation (MFV), Littlest Higgs with T parity (LHT)[2], Randall-Sundrum with custodial protection (RSc)[3], and four quark generations (SM4)[4]. It is interesting to note that tighter constraints on non-SM effects for $K_L \rightarrow \pi^0 \nu \bar{\nu}$ may be imposed by direct CP violation (ϵ'/ϵ), so that less than a factor of two enhancement in this branching ratio would be allowed[5].

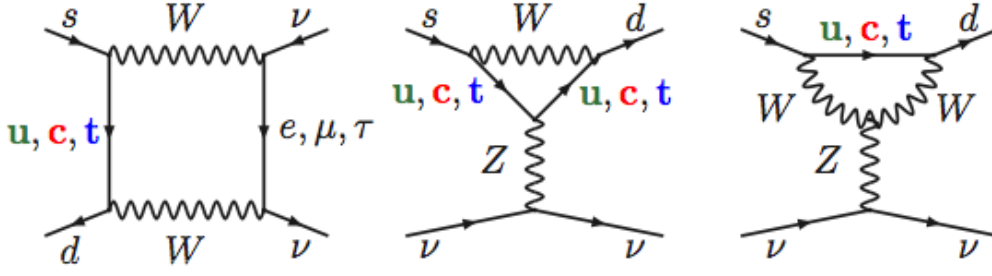


Figure 1: One-loop diagrams for $K \rightarrow \pi \nu \bar{\nu}$ decay.

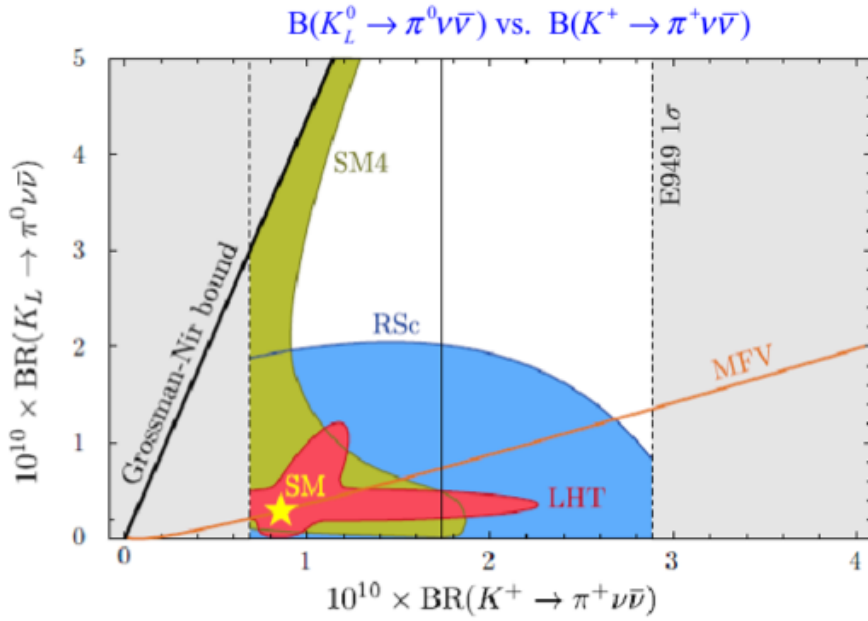


Figure 2: Figure courtesy of D.M. Straub[6]. Correlation between the branching ratios of $K_L \rightarrow \pi^0 \nu \bar{\nu}$ and $K^+ \rightarrow \pi^+ \nu \bar{\nu}$ in minimal flavor violation (MFV), and three concrete new physics models: Littlest Higgs with T parity (LHT)[2], Randall-Sundrum with custodial protection (RSc)[3], and four quark generations (SM4)[4]. The shaded area is ruled out experimentally at the 1σ level or model-independently by the Grossman-Nir bound[7]. The Standard Model point is marked by a star, and the central value of the BNL E787/E949 result[8] is indicated by the solid, vertical line.

3. $K^+ \rightarrow \pi^+ \nu \bar{\nu}$ Experimental History and Status

The first upper limit on the $K^+ \rightarrow \pi^+ \nu \bar{\nu}$ branching ratio was set by a heavy-liquid bubble chamber experiment in 1969[9]. The first $K^+ \rightarrow \pi^+ \nu \bar{\nu}$ event was seen at BNL by E787[10] in 1997. BNL E949 represented a significant upgrade from BNL E787; E949 detected four additional candidate events. The current branching ratio measurement,

$$B(K^+ \rightarrow \pi^+ \nu \bar{\nu}) = (17.3_{-10.5}^{+11.5}) \times 10^{-11}, \quad (3.1)$$

is a combined result based on the seven candidate events observed by the BNL E787 and E949 experiments[8]. The central value of the measured branching ratio is approximately twice that of the Standard Model prediction, but the measurement and prediction are consistent.

All $K^+ \rightarrow \pi^+ \nu \bar{\nu}$ experiments to date have used stopped kaons. The NA-62[11] experiment at CERN, currently under construction, will use a complementary decay-in-flight technique. In contrast to the stopped-kaon experiments, which have greater sensitivity at high π^+ momenta, the decay-in-flight technique is more sensitive to $K^+ \rightarrow \pi^+ \nu \bar{\nu}$ decays with lower π^+ momenta. NA-62 expects to see ~ 100 total $K^+ \rightarrow \pi^+ \nu \bar{\nu}$ events at the SM level and make a measurement of the $K^+ \rightarrow \pi^+ \nu \bar{\nu}$ branching ratio with precision of $\sim 10\%$.

ORKA is a proposed experiment to use the stopped-kaon technique and the FNAL Main Injector to detect ~ 1000 $K^+ \rightarrow \pi^+ \nu \bar{\nu}$ decays and make a measurement of the $K^+ \rightarrow \pi^+ \nu \bar{\nu}$ branching ratio with $\sim 5\%$ precision. The following section describes the stopped-kaon technique and the proposed ORKA experiment.

4. The ORKA Experiment

ORKA will use protons from the Main Injector (MI) at FNAL and will build on the BNL E949 detector design to measure the $K^+ \rightarrow \pi^+ \nu \bar{\nu}$ branching ratio with $\sim 5\%$ precision. Section 4.1 provides some details on the stopped-kaon technique and analysis of the BNL E787/E949 data. Plans to significantly improve on the sensitivity of the BNL experiments at ORKA are described in Sect. 4.2. Section 4.3 describes the breadth of physics measurements that may be made using the ORKA experiment. The status of the ORKA experiment is described in Sect. 4.4.

4.1 Stopped-Kaon Technique in BNL E787/E949

The ORKA detector design will be based on that of BNL E949, a schematic of which is shown in Fig. 3. Incoming K^+ particles are tracked, stop, and decay at rest in the scintillating-fiber stopping target. The momentum of the π^+ from $K^+ \rightarrow \pi^+ \nu \bar{\nu}$ decay is analyzed in the drift chamber. The π^+ stops in the range stack where its range and energy are measured and its decay products $\pi \rightarrow \mu \rightarrow e$ are detected. A straw chamber in the range stack provides additional information on the π^+ position. An extensive veto system provides 4π photon veto coverage. The entire detector is immersed in a 1 T solenoidal magnetic field along the beam direction.

Measurement of the $K^+ \rightarrow \pi^+ \nu \bar{\nu}$ branching ratio at the 10^{-10} level is challenging because the signal, consisting only of the $\pi \rightarrow \mu \rightarrow e$ decay chain, is poorly defined and the background, primarily from K^+ decays with branching ratios as much as ten orders of magnitude larger than $K^+ \rightarrow \pi^+ \nu \bar{\nu}$ decay, is large and difficult to distinguish from the signal. Figure 4 (left panel) shows the momentum spectrum of the outgoing charged particle for $K^+ \rightarrow \pi^+ \nu \bar{\nu}$ signal and important K^+ -decay background sources. To suppress background to a sufficiently low level, the detector must have excellent π^+ particle identification to reject background from $K^+ \rightarrow \mu^+ \nu_\mu$ and $K^+ \rightarrow \mu^+ \nu_\mu \gamma \gamma$ decays, highly efficient 4π solid-angle photon veto coverage to reject background from $K^+ \rightarrow \pi^+ \pi^0$ decays, and a K^+ identification system to remove beam-related background.

Figure 4 (left panel) also shows two kinematic regions that can be used to search for $K^+ \rightarrow \pi^+ \nu \bar{\nu}$ decay in the data; these regions are chosen to avoid background. In the PNN1 region, the π^+ momentum lies between the π^+ momentum from $K^+ \rightarrow \pi^+ \pi^0$ decay and the π^+ kinematic limit of

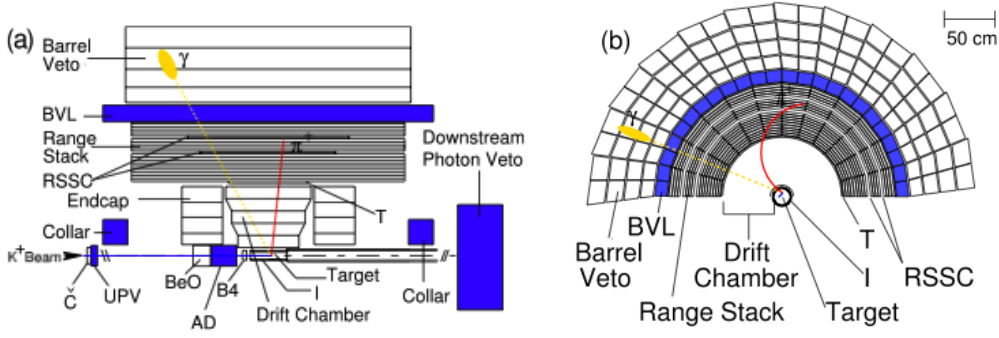


Figure 3: Schematic side (a) and end (b) views of the upper half of the BNL E949 detector. An incoming K^+ traverses all the beam instruments, stops, and decays. The outgoing π^+ and one photon from $\pi^0 \rightarrow \gamma\gamma$ are also shown.

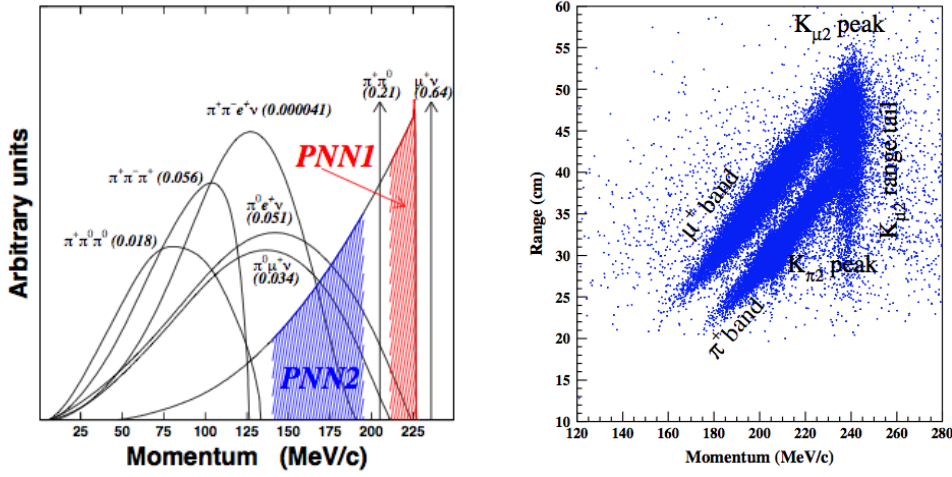


Figure 4: (left) π^+ (or μ^+) momentum distributions for several K^+ decay modes. The respective branching ratios are shown in parentheses. The signal regions used for the E787 and E949 $K^+ \rightarrow \pi^+ \nu \bar{\nu}$ branching ratio analyses (PNN1 and PNN2) are indicated. (right) Range in plastic scintillator vs. momentum for charged particles accepted by the $K^+ \rightarrow \pi^+ \nu \bar{\nu}$ PNN1 trigger. The concentrations of events resulting from two-body decays are labeled “ $K_{\pi 2}$ peak” and “ $K_{\mu 2}$ peak.” The decays $K^+ \rightarrow \pi^0 \mu^+ \nu_{\mu}$ and $K^+ \rightarrow \mu^+ \nu_{\mu} \gamma$ contribute to the muon band. The pion band results from $K^+ \rightarrow \pi^+ \pi^0 \gamma$ decay in which the π^+ scatters in the target or range stack and beam π^+ that scatter in the target.

227 MeV/c. The μ^+ momentum from $K^+ \rightarrow \mu^+ \nu_{\mu}$ decay lies above the π^+ kinematic limit. In the PNN2 region, the π^+ momentum is below that from $K^+ \rightarrow \pi^+ \pi^0$ decay, but analysis of this region is complicated by having additional sources of background from three-body decays of the K^+ . Beam related background, in which a K^+ decays in flight, a beam π^+ scatters in the stopping target, or a K^+ undergoes charge exchange, must also be considered. Figure 4 (right panel) shows the range and momentum of the charged particle for all events passing the PNN1 trigger. Background from $K^+ \rightarrow \pi^+ \pi^0$, $K^+ \rightarrow \mu^+ \nu_{\mu}$, various 3-body decays, and scattered pions are identified.

Data from BNL E787/E949 are shown in Fig. 5. Data in the PNN1 and PNN2 regions were analyzed separately. The analysis was done using a blind signal region. The final background

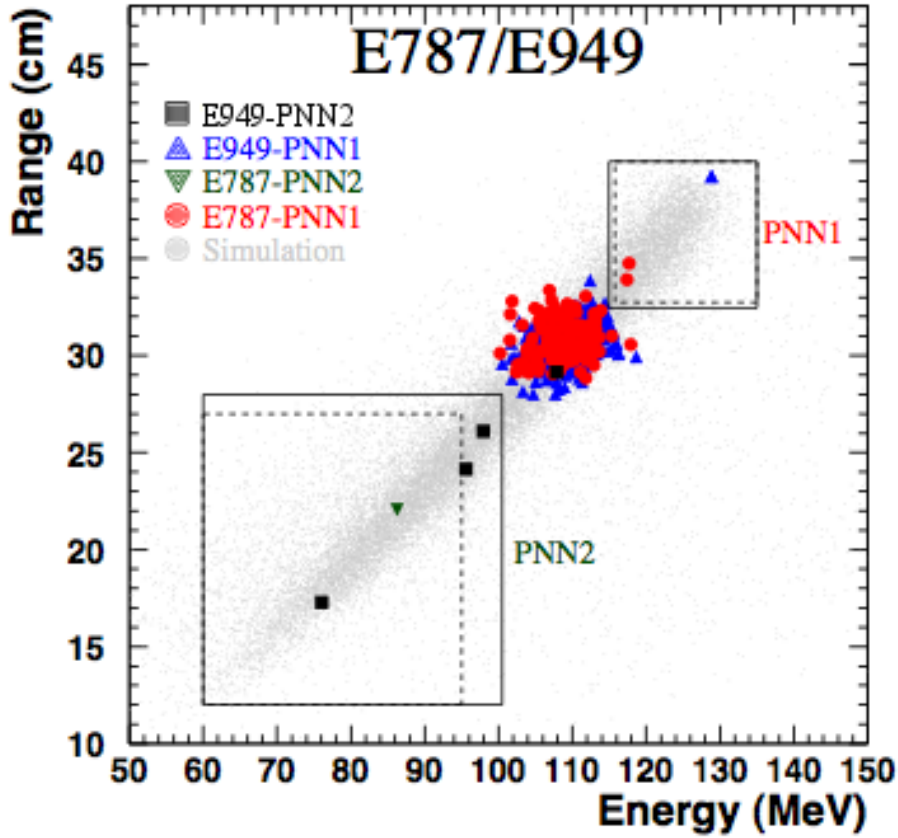


Figure 5: Range vs. kinetic energy for events satisfying all other selection criteria in BNL E787/E949. The two signal regions, PNN1 and PNN2, are shown by the dashed line (E787) and the solid line (E949). Events near $E = 108$ MeV are background from $K^+ \rightarrow \pi^+ \pi^0$ decays which are not removed by photon veto requirements. The light points represent the expected distribution of $K^+ \rightarrow \pi^+ \nu \bar{\nu}$ events from simulation.

estimates were obtained from different data samples than were used to determine the selection criteria, using 2/3 and 1/3 of the data respectively, and the background level was evaluated based on information from outside the signal region. The expected number of background events was $\ll 1$ in PNN1 and ~ 1 in PNN2. As seen in Fig. 5, a total of seven candidate $K^+ \rightarrow \pi^+ \nu \bar{\nu}$ events were identified.

4.2 ORKA Sensitivity

The ORKA experiment will have a sensitivity ~ 100 times that of BNL E949. The beam line will provide one factor of ten, while increases in detector acceptance provide the other order of magnitude.

The ORKA experiment intends to extract a 95-GeV beam from the MI ring onto a production target, select a 600-MeV/c K^+ beam from that target, and bring the kaons to rest at the center of the detector. The FNAL MI provides $\sim 25\%$ fewer protons per spill than the BNL beam. However, ORKA's kaon beam line provides a factor of >4 times the number of kaons per proton from a

longer target, increased angular acceptance, and increased momentum acceptance. The beam-line design also allows a 40% increase in the fraction of kaons that survive until the stopping target and an additional factor of 2.6 in the fraction of kaons that come to rest in the stopping target. The detector will operate at a higher instantaneous rate, which leads to $\sim 10\%$ more losses from vetoed events. Overall, the ORKA beam line will provide ten times more $K^+ \rightarrow \pi^+ \nu \bar{\nu}$ events than BNL E949.

The ORKA detector, the design of which is modeled closely on that of BNL E949 (see Fig. 3), will have a factor of ten greater acceptance than the BNL E949 detector. Most of the increases in acceptance are incremental; a variety of improvements to the detector design each provide acceptance increases of 6-60%. The largest change in acceptance is a factor of 2.2 increase in the $\pi \rightarrow \mu \rightarrow e$ acceptance, which is the result of several features of the ORKA detector. The ORKA range stack has increased segmentation relative to the range stack in BNL E949; this will reduce losses from accidental activity and improve π/μ particle identification. ORKA will use higher quantum efficiency photo-detectors and/or better optical coupling to increase the scintillator light yield, which will improve μ identification. ORKA will also employ a modern, deadtime-less DAQ and trigger so that losses from online π/μ particle identification will be eliminated. The irreducible losses to $K^+ \rightarrow \pi^+ \nu \bar{\nu}$ acceptance are from necessary cuts on the measured π^+ and μ^+ lifetimes and from μ^+ and e^+ particles that do not deposit enough energy to be detected. In the PNN1 region, the $\pi \rightarrow \mu \rightarrow e$ acceptance in ORKA is estimated to be $\sim 78\%$.

Preliminary simulation of the ORKA detector for optimization of the detector design is underway. Figure 6 shows an ILCroot[12] event display of the ORKA detector in which a $K^+ \rightarrow \pi^+ \pi^0$ decay has been simulated.

The ORKA experiment will detect ~ 210 $K^+ \rightarrow \pi^+ \nu \bar{\nu}$ events per year at the Standard Model level. Figure 7 shows the fractional error on the $K^+ \rightarrow \pi^+ \nu \bar{\nu}$ branching ratio as a function of running time. ORKA expects to reach the projected theoretical uncertainty on the $K^+ \rightarrow \pi^+ \nu \bar{\nu}$ branching ratio after taking data for about five years.

4.3 Physics Breadth in ORKA

The ORKA detector is highly optimized for detection of $K^+ \rightarrow \pi^+ \nu \bar{\nu}$ decay; the signal for this decay is basically $K^+ \rightarrow \pi^+$ plus missing energy. In the case of $K^+ \rightarrow \pi^+ \nu \bar{\nu}$ decay, the missing energy is neutrinos, but other forms of missing energy can be sought by observing the shape of the π^+ spectrum. For this reason, ORKA will have sensitivity to many modes of considerable interest. It is also true that a very large number of stopped kaons will decay in the ORKA detector. The sheer volume of data may facilitate measurements even in decay modes for which the detector is not optimized.

One possible source of missing energy is the case in which a single unseen particle recoils from the π^+ . In this case, the π^+ spectrum is a peak and its width is determined by the detector resolution. Theoretical models exist in which the unseen X^0 is a familon[13], an axion[14], a light scalar pseudo-Nambu-Goldstone boson[15], a sgoldstino[16], a gauge boson (A') corresponding to a new U(1) gauge symmetry [17, 18], or a light dark-matter candidate[19, 20, 21].

ORKA will have sensitivity to many other interesting decay modes. These include: $K^+ \rightarrow \pi^+ \pi^0 \nu \bar{\nu}$, $K^+ \rightarrow \pi^+ \gamma$, $K^+ \rightarrow \mu^+ \nu_{heavy}$, $K^+ \rightarrow \pi^+ \gamma \gamma$, $\pi^0 \rightarrow \nu \bar{\nu}$, and $\pi^0 \rightarrow \gamma X^0$. There are other

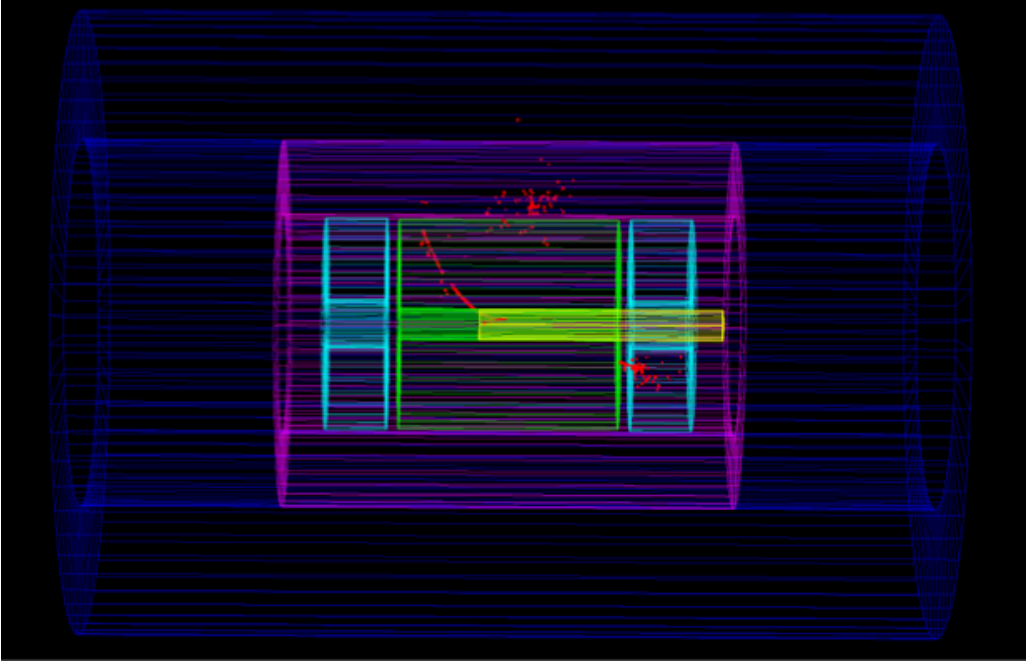


Figure 6: Event display from ILCroot simulation of the ORKA detector. The target is shown in yellow, the drift chamber in green, the range stack in pink, the barrel veto in blue, and the veto end-caps in cyan. The simulated event is a $K^+ \rightarrow \pi^+ \pi^0$ decay. The two photon clusters from π^0 decay and the $\pi^+ \rightarrow \mu^+$ tracks are visible.

possible searches, such as $K^+ \rightarrow \pi^+ A'$, $A' \rightarrow e^+ e^-$, for which the ORKA detector is not optimized, but might still have sensitivity because of the large numbers of stopped-kaon decays.

ORKA will also be able to make precise measurements of important kaon branching ratios and fundamental parameters. $R_K = \Gamma(K^+ \rightarrow e^+ \nu_e) / \Gamma(K^+ \rightarrow \mu^+ \nu_\mu)$ has been measured to 0.4% by NA-62[22]. ORKA will be able to measure this ratio with <0.1% statistical precision; study of the expected systematic uncertainty is still needed. Other fundamental kaon measurements accessible to ORKA include the K^+ lifetime and the $B(K^+ \rightarrow \pi^+ \pi^0) / B(K^+ \rightarrow \mu^+ \nu_\mu)$ ratio.

4.4 Status of ORKA

The ORKA collaboration submitted a proposal[23] to FNAL in November 2011. The experiment received Stage 1 approval from the FNAL directorate in December 2011. The planned site for the experiment is B0, so that ORKA can re-use the CDF solenoid, cryogenics, and infrastructure. The ORKA detector is being designed to fit inside the CDF solenoid. Decommissioning of CDF in a way that facilitates eventual use of CDF hall by ORKA is underway; this effort is being funded in the FY13 FNAL budget. Plans are being made and beam-line elements are being identified for a beam line to transport protons from the Main Injector extraction point to B0 in the Tevatron tunnel. A preliminary design for the kaon beam line from the production target to the detector has been simulated and is being refined. Research and development on detector design has begun. The ORKA collaboration consists of 17 institutions from six countries. Because ORKA is a fourth generation detector, building on experience from BNL E787/E949, an aggressive construction schedule is thought possible; the collaboration expects to begin taking data within five years of

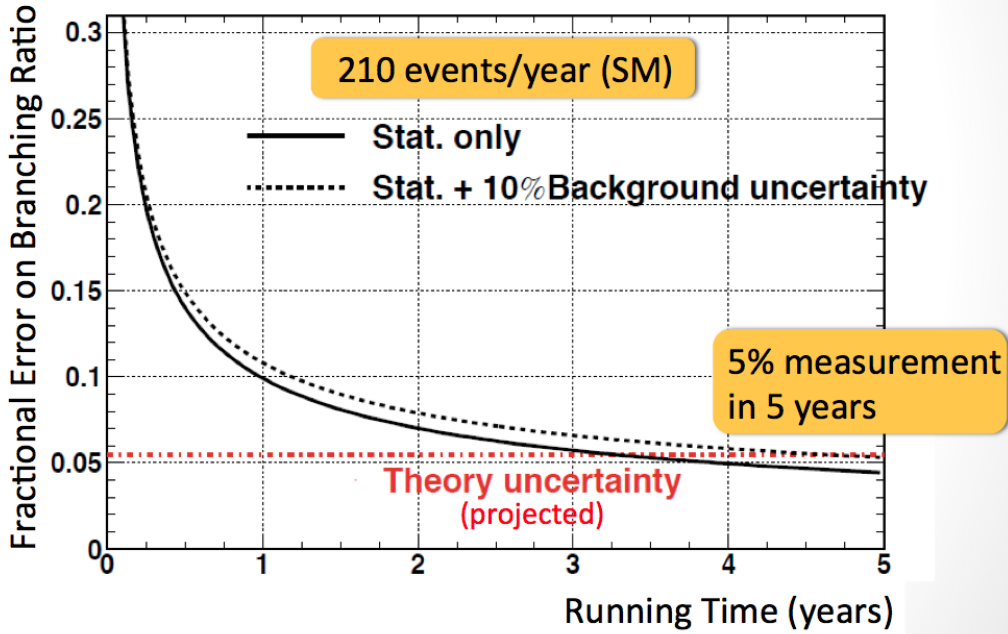


Figure 7: The fractional uncertainty in the ORKA measurement of the $K^+ \rightarrow \pi^+ \nu \bar{\nu}$ branching ratio as a function of running time. The solid (dashed) curve is the sensitivity assuming no (10%) background uncertainty. The flat dashed line is the uncertainty in the theoretical prediction of the $K^+ \rightarrow \pi^+ \nu \bar{\nu}$ branching ratio, excluding uncertainties in the CKM matrix elements.

funding approval. The ORKA collaboration is working with the DOE to determine when funding will be available.

5. Summary

Precision measurement of the $K^+ \rightarrow \pi^+ \nu \bar{\nu}$ branching ratio is an opportunity to search for the effects of new physics at and beyond the mass scale accessible by direct searches. The ORKA experiment will use proven accelerator technology, detector technology, and experimental techniques to measure the $K^+ \rightarrow \pi^+ \nu \bar{\nu}$ branching ratio with an uncertainty of $\sim 5\%$, allowing 5σ -level detection of deviations from the Standard Model as small as 35%. The ORKA experiment will make use of protons from the FNAL Main Injector and will be sited at B0 at Fermilab. The collaboration is currently conducting detector R&D in preparation for ORKA.

References

- [1] J. Brod *et al.* *Phys. Rev. D*, vol. 83, p. 034030, 2011.
- [2] M. Blanke *et al.* *Acta Phys. Polon. B*, vol. 41, p. 637, 2010.
- [3] M. Blanke *et al.* *JHEP*, vol. 0903, p. 108, 2009.
- [4] A. Buras *et al.* *JHEP*, vol. 1009, p. 106, 2010.

- [5] U. Haisch in *Project X Physics Study*, 2012.
<https://indico.fnal.gov/getFile.py/access?contribId=22&sessionId=5&resId=0&materialId=slides&confId=5276>.
- [6] D. Straub in *Proceedings of CKM2010, the 6th International Workshop on the CKM Unitarity Triangle, University of Warwick, UK 6-10 September 2010*.
- [7] Y. Grossman and Y. Nir *Phys. Lett. B*, vol. 398, p. 163, 1997.
- [8] A. Artamonov *et al. Phys. Rev. D*, vol. 79, p. 092004, 2009.
- [9] U. Camerini *et al. Phys. Rev. Lett.*, vol. 23, p. 326, 1969.
- [10] S. Adler *et al. Phys. Rev. Lett.*, vol. 79, p. 2204, 1997.
- [11] “2013 NA62 status report to the CERN SPSC.”
<https://na62.web.cern.ch/na62/Documents/CERN-SPSC-2013-009.pdf>.
- [12] <http://www.dmf.unisalento.it/~danieleb/IlcRoot/>.
- [13] F. Wilczek *Phys. Rev. Lett.*, vol. 49, p. 1549, 1982.
- [14] M. Hindmarsh and P. Moulatsiotis *Phys. Rev. D*, vol. 59, p. 055015, 1999.
- [15] T. Banks and H. Haber *JHEP*, vol. 0911, p. 097, 2009.
- [16] D. Gorbunov *Nucl. Phys. B*, vol. 602, p. 213, 2001.
- [17] T. Aliev *et al. Nucl. Phys. B*, vol. 335, p. 311, 1990.
- [18] M. Pospelov *Phys. Rev. D*, vol. 80, p. 095002, 2009.
- [19] M. Pospelov *et al. Phys. Lett. B*, vol. 662, p. 53, 2008.
- [20] P. Fayet *Phys. Rev. D*, vol. 75, p. 115017, 2007.
- [21] J. Gunion *et al. Phys. Rev. D*, vol. 73, p. 015011, 2006.
- [22] C. Lazzeroni *et al. Phys.Lett.B*, vol. 719, pp. 326–336, 2013.
- [23] J. Comfort *et al.*, “Fermilab-proposal-1021.” http://www.fnal.gov/directorate/program_planning/Dec2011PACPublic/ORKA_Proposal.pdf.